Dalton Transactions

ROYAL SOCIETY OF CHEMISTRY

COMMUNICATION

View Article Online
View Journal | View Issue

Cite this: *Dalton Trans.*, 2020, **49**, 14781

Received 7th September 2020,
Accepted 9th October 2020

DOI: 10.1039/d0dt03129a

rsc.li/dalton

An approach to estimate the barrier height for magnetisation reversal in {Dy_2} SMMs using *ab initio* calculations†

Sourav Dey and Gopalan Rajaraman *

Although *ab initio* CASSCF calculations yield a good numerical estimate of barrier height for magnetisation reversal for mononuclear Dy(III) SIMs, obtaining a reliable value for higher nuclearity clusters such as {Dy_2} are challenging. By analysing *ab initio* computed data of thirty-one different {Dy_2} SMMs, we propose a model equation that relates the calculated barrier heights to the experimental values and offers a viable way to predict the barrier heights in {Dy_2} SMMs.

Single-molecule magnets (SMMs) have gained significant attention in recent years due to potential applications proposed for them in the area of information storage, spintronics and quantum computing.[1,2–5] The two key parameters that control the magnetic properties of SMMs are the barrier height for the magnetisation reversal (U_{eff}) and the blocking temperature (T_B). Several important breakthroughs were achieved in the last three years in this area, where the T_B values were raised from liquid helium (T_B > 4 K) to liquid nitrogen temperatures (T_B < 77 K with a sweep rate of 22 Oe s^{-1}).[6,7] Despite concentrated efforts by several research groups, the value of T_B has not scaled with U_{eff} values. This is due to various pathways available for relaxation of magnetisation such as quantum tunnelling of magnetisation (QTM), Raman process, molecular vibrations *etc*. that undercut the Orbach relaxation pathways. In this area, Dy(III) based magnets are the most attractive and recent reports suggest that the axial limit that is correlated to the U_{eff} values are already breached, while it may be still possible to enhance this further *via* other ligand/methods.[6,7] An alternative way to enhance the U_{eff}/T_B, would be to shift to the dinuclear framework, where intramolecular exchange coupling between lanthanide ions could suppress the QTM to a certain extent and can offer larger U_{eff} and T_B values. There are many examples to this effect that demonstrate the potent of {Dy_2}/{Ln_2} motif in obtaining attractive U_{eff} and T_B values.[8–10]

Ab initio calculations based on CASSCF/RASSI-SO/SINGLE_ANISO methods played an important role in the design and development of mononuclear Ln(III) SMMs. These methods offer insight into the nature of magnetic anisotropy, clues on the mechanism of magnetic relaxation and have been used extensively to make viable predictions.[11] In this regard, Aravena has proposed a model equation to calculate the U_{eff} for high-performance Dy(III) SIMs exhibiting good agreement with experiments.[12] A year later, the Chilton and Aravena groups also proposed a correlation of T_B with the relaxation mechanism in high-performance monometallic Dy(III) SIMs.[13,14] Though significant efforts have been undertaken to probe the relaxation mechanism of mononuclear Dy(III) SIMs, studies on the relaxation mechanism of polynuclear complexes are rare.[15–18] As the exchange coupling between the Dy(III) ions is cumbersome to estimate, the barrier heights estimated from theoretical calculations (U_{cal}) are often substantially different from the experimental U_{eff} values. While the U_{cal} value computed for mononuclear Dy(III) ion agree with U_{eff} values for some {Dy_2} dimer,[19,20] this is not true for the majority of the examples.[21,22]

To offer insight into this subject, here we have attempted to develop a correlation between U_{cal} and U_{eff} values by thoroughly looking at the mechanism of relaxation in thirty-one non-radical {Dy_2} SMMs (with U_{eff} ranges from 20 to 860 cm^{-1}) reported in the literature.[8] While radical bridged {Dy_2} are very attractive for SMMs as they offer stronger Dy(III)-radical exchange, we have not included them in our studies as the type of exchange involved is very different (direct *vs*. superexchange) in this class, and only limited experimental/computed data is available. Further, we have restricted our studies to {Dy_2} dimers where complete characterisation, including the qualitative mechanism of magnetisation relaxation from *ab initio* calculations, are available (see ESI† for structures).[10,23] For convenience, these {Dy_2} SMMs have been

Department of Chemistry. Indian Institute of Technology Bombay, Powai, Mumbai, 400076, India. E-mail: rajaraman@chem.iitb.ac.in

†Electronic supplementary information (ESI) available: Structures of 31 {Dy2} SMM along with energy spectrum, *g* tensor of selected 3 complexes. See DOI: 10.1039/d0dt03129a

classified into five categories where *class (a) {Dy_2} dinuclear motifs with metallocene ligand backbone*: dinuclear metallocene complexes are known prior to the popular mononuclear Dy(III) SIMs that are reported to possess large T_B values.[7] Nine complexes are studied in this class (complex **1–9**, Fig. 1a, S1–S9†) which shows a large variation in the U_{eff} from 26 to 860 cm^{-1} (Tables 1 and S1†). The latest discovery in this class is [{Dy$(Cp^*)_2(\mu\text{-}Me_3AlNEt_3)\}_2$][Al{$OC(CF_3)_3\}_4]_2$ (**9**, Cp^* = C_5Me_5, Fig. 1a) complex which is reported to have U_{eff} value of 860 cm^{-1} with T_B of 12 K.[19] *Class (b) {Dy_2} dinuclear motif having Schiff base ligands*: Schiff base ligands which can coordinate with multiple Dy(III) centres have produced a large number of SMMs. A total of thirteen complexes (**10–22**, Fig. S10–S22†) has been chosen in this class which shows smaller U_{eff} values (Tables 1 and S1†) compared to class (a) type complexes. The largest U_{eff} value of 104.2 (FR) and 137.7 (SR) cm^{-1} has been achieved in $[Dy_2(ovph)_2Cl_2(MeOH)_3]$ (**15**, Fig. 1b, H_2ovph = pyridine-2-carboxylic acid [(2-hydroxy-3-methoxyphenyl)methylene] hydrazide) complex.[22] *Class (c) {Dy_2} dinuclear motif having organometallic building blocks*: Murugesu and co-workers introduced organometallic rings in between two Dy(III) ions to achieve strong magnetic exchange. Two complexes (**23–24**, Fig. S23 and 24†) are chosen in this class, which shows even smaller U_{eff} values compare to class (b) (Tables 1 and S1†). *Class (d) {Dy_2} dinuclear motif having a bridging group H^-, and Cl^-*: the complexes with bridging groups H^- and Cl^- are included in this class which does not have cyclopentadienyl, Schiff base or organometallic building blocks. Two complexes (**25–26**, Fig. S25–26†) are chosen in this class. In class d, the large U_{eff} of 433 cm^{-1} was achieved in [Dy$(Cy_2N)_2(\mu\text{-}Cl)(THF)]_2$ (**26**, Fig. 1c) in which the low coordinate Dy(III) centres are ferromagnetically coupled.[20] *Class (e) {Dy_2} dinuclear motif having* 2,2′-bipyrimidine as a bridging group: there are five complexes (**27–31**, Fig. S27–31†) reported in this category with the neutral 2,2′-bipyrimidine as bridging group yielding the U_{eff} values in the range of 23 to 185 cm^{-1}.

While the Dy(III) SIM with metallocene ligand backbone provides the largest blocking barrier for magnetisation reversal, the {Dy_2} SMMs have comparatively lower U_{eff} values and this due to presence of equatorial ligand(s) which connects the

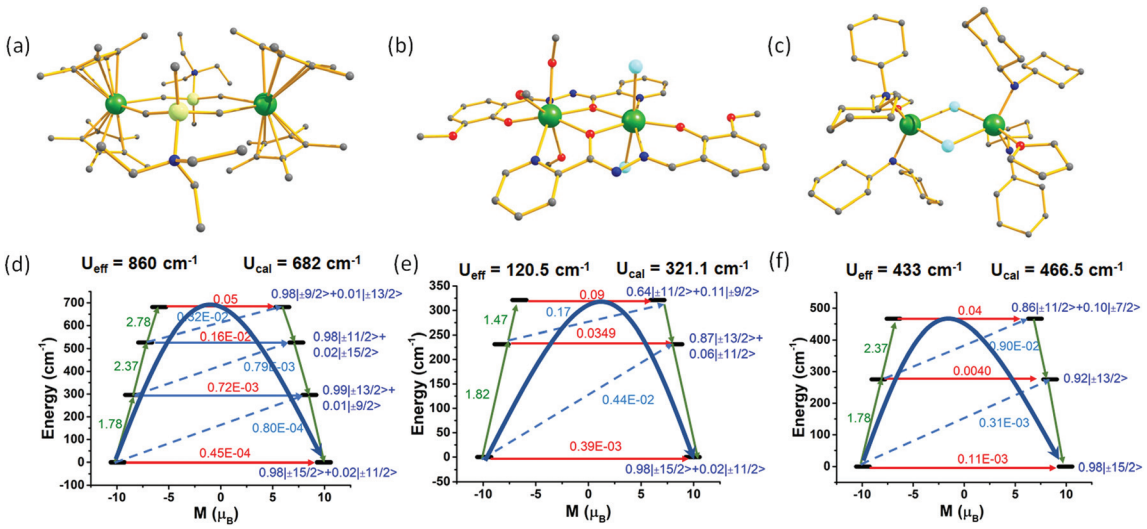

Fig. 1 (a–c) Molecular structures of the best SMM in the class of a (**9**), b (**15**) and d (**26**). Colour code: Dy-green, Cl-aqua, Al-lime, O-red, N-blue, C-grey. Hydrogens are omitted for clarity. (d–f) Mechanism of relaxation reported for complexes **9**, **15** and **26**, respectively. The red arrows indicate the QTM or TA-QTM *via* ground or excited KD, respectively. The blue characters indicate the composition of m_J of a KD. The sky dotted arrows shows the mechanism of Orbach process. The olive arrows indicate the pathway of magnetic relaxation. The large blue arrow represents mechanism overall of magnetic relaxation.

Table 1 Selected examples of {Dy_2} SMMs with reported U_{eff} values along with *ab initio* calculated values (all values in cm^{-1}). The QTM/TA-QTM of the $(x-1)^{th}$ KD has been provided if it relaxes *via* x^{th} KD. Full list of all complexes is given in Table S1†

Class	Complex (CSD ref code)	U_{eff}	U_{cal1}	U_{cal2}	QTM/TA-QTM (Dy1)	QTM/TA-QTM (Dy2)	J	U_{caleff}	Ref.
a	8 (VUQHIB)	330.0	462.0	462.0	0.0026	0.0026	0.001	355.4	24
a	9 (HULRAK)	860.0	680.8	680.8	0.0016	0.0016	0.420	857.3	19
b	18 (TIJJAA)	54.0	196.1	196.1	0.0067	0.0067	0.088	59.8	25
c	24 (SENJON)	40.2[a]	115.9	69.1	0.0047	0.0019	0.781	72.7	26
d	26 (GOMTIO)	433.0	466.5	466.5	0.0040	0.0040	−0.018	233.0	20
e	28 (YUDBUX)	38.2[a]	141.9	129.9	0.0034	0.0100	0.004	54.8	15

[a] The U_{eff} value in Table 1 was taken from the average from the two-relaxation process called FR and SR.

two metal centres and reduces the axiality of the complexes. For this reason, the weakly bound Dy(III) complexes in the class (a) shows larger U_{eff} values compared to other classes. For classes (b), (c) and (e), the smaller single-ion anisotropy of the individual Dy(III) ion and the magnetic exchange between the Dy(III) ion found to be the determining factor that controls the U_{eff} values. The smaller single-ion anisotropy in these class originates from the weaker ligand coordination and strong structural distortions from desired symmetries. The complexes in class (d) contain Dy(III) ion in a low coordinate environment which provides large single-ion anisotropy resulting in larger U_{eff} values with the exception of complex **25** (Fig. S25†) where a stronger hydride donor as bridging ligand diminish the single-ion anisotropy. The CASSCF/RASSI-SO/SINGLE_ANISO computed energy barrier of individual Dy(III) centres, QTM/TA-QTM probability and exchange values (total *J*, within Lines model) for selected complexes in classes a–e are provided in Table 1 with the full list is given in ESI (Table S1†).

We have computed the mechanism of magnetisation relaxation for individual Dy(III) ion complexes using the CASSCF/RASSI-SO/SINGLE_ANISO approach using the reported computational methodology (Fig. 1d–f for complex **9**, **15** and **26**, see ESI† for computational details and relaxation mechanism of other complexes). Complex **9** found to relax *via* third excited KDs while complexes **15** and **26** found to relax *via* second excited KDs due to significant TA-QTM and deviation of the anisotropy axis with the ground state at this level (see Tables S2–S5† for computed energy and *g* tensor). While the computed U_{cal} value matches with U_{eff} value in **26**, there is a strong deviation observed in **9** and **15**. In most of the $\{Dy_2\}$ SMM, the U_{eff} does not show any agreement with barrier estimated based on single-ion anisotropy (U_{cal}) (Tables 1 and S1†). Further, in many cases, even the exchange-coupled energy barrier is far off compared to the experimental estimates.[16,17]

To understand this in detail, we have analysed various *ab initio* computed parameters with the U_{eff} values, and these are given in Tables 1 and S1 in ESI.† From the data, it has been found that the U_{eff} is (i) proportional to the U_{cal} value of the individual Dy(III) centres and (ii) inversely proportional to QTM of the ground state of individual metal centres if it relaxes *via* first excited KD or TA-QTM of the $(x-1)^{th}$ KD if it relaxes *via* x^{th} higher excited KDs other than first excited KD. The magnetic exchange (*J*, obtained from the fitting of temperature and field-dependent magnetisation) acts as a perturbation in the magnetisation relaxation. By analysing all the computed parameters, we propose the following empirical model equation (eqn (1)).

$$U_{caleff} = \left[\frac{U_{cal1}}{(QTM/TA\text{-}QTM)\times 10^3} + \frac{U_{cal2}}{(QTM/TA\text{-}QTM)\times 10^3}\right] + 15J \quad (1)$$

where U_{cal1} and U_{cal2} is the *ab initio* CASSCF/RASSI-SO/SINGLE_ANISO calculated blocking barrier for Dy1 and Dy2 centres, respectively. This equation takes into consideration the computed QTM/TA-QTM probabilities in obtaining a blockade barrier. Furthermore, the U_{cal} values are derived from the crystal field splitting of m_J levels, and the QTM/TA-QTM probabilities are computed using g-anisotropy, and therefore, they could not be compared directly. Besides QTM/TA-QTM values smaller than $10^{-3}\mu_B$ are considered very small and can be considered negligible.[27] To account for this cut-off value of QTM/TA-QTM probability, we have used a prefactor of 10^3 in our equation. In addition to this, we have also included the exchange coupling constant *J* in our equation. As the *J* values are very small for Dy(III) dimers, we have used the gap between the high-spin and low-spin state of Dy(III). *i.e.* 15*J*, in our equation.[28] This equation considers the single-ion anisotropy of both the Dy(III) centres, QTM/TA-QTM probabilities as well as the *J* values (total *J* since the nature of the ground state depends on total *J* value[29]) to arrive at a new computed barrier height (termed as U_{caleff}) that correlate well with the experimental U_{eff} values in $\{Dy_2\}$ SMM.[32]

Using eqn (1), we have estimated the U_{caleff} from the *ab initio* computed parameters for all the thirty-one dimers reported and these are listed in Tables 1 and S1.† Except for one example (complex **7**), there is a one to one correlation between experimental U_{eff} values and the U_{caleff} obtained using eqn (1). In particular for complex **2**, the U_{cal} value estimated is 383.4 cm^{-1} which is significantly overestimated compare to U_{eff} value of 26 cm^{-1}. For this complex, U_{caleff} is estimated to be 50.3 cm^{-1}, and this unveils the level of improvement in the estimation of barrier height in $\{Dy_2\}$ system using eqn (1). Similarly, the U_{cal} values of complexes **10–13**, **15–22** in class (b) (see Table 1 and Table S1†) are overestimated by more than 100 cm^{-1} compare to experimental U_{eff} values. The U_{caleff}, on the other hand, minimise the deviation significantly. For complex **18**, the U_{cal1} (Dy1) and U_{cal2} (Dy2) are overestimated by more than 100 cm^{-1} compare to U_{eff} values while the U_{caleff} improves the estimate significantly. A similar trend is visible also for class (c) complexes where U_{caleff} matches U_{eff} better compare to U_{cal}. The U_{cal} value of the complexes in class (d) is, in general, agree well with U_{eff} values estimated with the exception of complex **25** (Table S1†). The U_{cal1} and U_{cal2} of complex **25** are found to be 94 and 231 cm^{-1}, respectively both of which are largely overestimated compare to U_{eff} of 40 cm^{-1}. The U_{caleff} of complex **25** is estimated to be 29.9 cm^{-1}, and this agrees much better with experiments compared to single-ion barrier height. The overestimation of U_{cal} compare to U_{eff} is also found class (e) complexes (with the exception **30**). The estimated U_{cal} (Dy1) and U_{cal} (Dy2) of complex **29** are 183.8, and 157.4 cm^{-1}, respectively which is overestimated compare to U_{eff} of 93.1 cm^{-1}.[15] The exchange-coupled energy barrier is available in this case, and this is reported to be 128.0 cm^{-1}. Although this value is closer to U_{eff} value compare to single-ion barrier height, the deviations are visible. For complex **29** the U_{caleff} value is estimated to be 92.6 cm^{-1}, and this is in excellent agreement with the experimental U_{eff} values. Thus this empirical model equation not only yields a very good estimate of barrier height for magnetisation reversal for complexes which are closer to single-ion Dy(III) barrier heights but

also yield the best estimate when these values diverge significantly, thus offering an approach to compute barrier height reliably for $\{Dy_2\}$ dimers using *ab initio* calculations. Although the values computed are certainly better than the value obtained from single-ion anisotropy or even the one obtained for the dinuclear framework, the agreement between U_{eff} and U_{caleff} are less than satisfactory in some cases. Particularly for complexes **26** and **30**, the deviations are high. Experimental studies indicate that Raman process is the dominant mechanism of relaxation in these cases, as there are no Raman terms in our equation, larger deviations are expected.[20,22,30] There is an only limited number of examples known with dominant Raman relaxation, and therefore suitable modification could not be performed at present.

Further on, as U_{caleff} yield a good numerical estimate of U_{eff} values in $\{Dy_2\}$ dimers, we have explored the relationship between the two sets. A linear relationship offering excellent fit (complex **7** and **26** are outliers, hence they are not been considered in the fitting) between these two parameters is obtained (Fig. 2). To check the validity of this equation further, we have chosen, $\{Dy_2\}$ SMM, $[\{Dy(BH_4)_2(THF)\}_2(Fv^{tttt})]$ (**32**, Fv^{tttt} = $[1,1',3,3'\text{-}(C_5{}^tBu_2H_2)_2]^{2-}$, Fig. S33†) reported by Layfield and co-workers very recently.[31] The complex **32** is found to relax *via* first excited KD (176 cm^{-1} for Dy1 and 181 cm^{-1} for Dy2). For this complex, the U_{caleff} is estimated to be 144.1 cm^{-1}, and the linear regression equation yield a value 150.5 cm^{-1} both these values are in excellent agreement with the experimental U_{eff} value of 154 cm^{-1} offering confidence on the predictive potential of the proposed equation.

To this end, by carefully analysing thirty-one different $\{Dy_2\}$ dimers, we have proposed an empirical equation that takes into account the single-ion anisotropy of the Dy(III), QTM/TA-QTM probabilities and the exchange coupling between the two Dy(III) ions to estimate the barrier height for magnetisation reversal. The theoretical barrier height estimated using this equation is in excellent agreement with experimental values, unlocking the possibility of utilising the *ab initio* methods to compute barrier heights reliably in $\{Dy_2\}$ and possibly other polynuclear complexes.

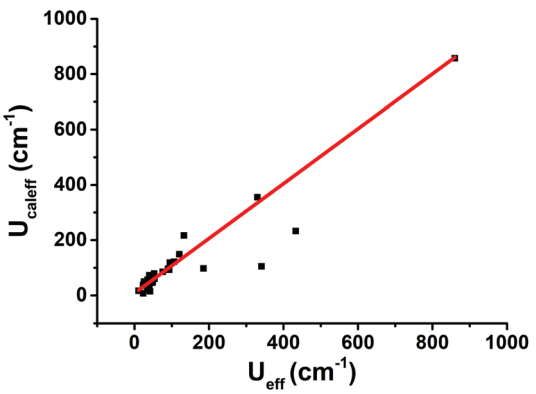

Fig. 2 Comparison of U_{eff} with the U_{caleff} from model eqn (1). A good linear fit (slope = 0.99 and intercept = 7.82) is obtained with R^2 = 0.97.

Conflicts of interest

There are no conflicts to declare.

Acknowledgements

S. D. would like to thank UGC for SRF fellowship and IIT Bombay for CRAY supercomputing facility. GR would like to thank DST/SERB (CRG/2018/000430, DST/SJF/CSA03/2018-10; SB/SJF/2019-20/12) for funding.

Notes and references

1 R. Sessoli, D. Gatteschi, A. Caneschi and M. Novak, *Nature*, 1993, **365**, 141–143.
2 M. Atzori, L. Tesi, E. Morra, M. Chiesa, L. Sorace and R. Sessoli, *J. Am. Chem. Soc.*, 2016, **138**, 2154–2157.
3 J.-L. Liu, Y.-C. Chen and M.-L. Tong, *Chem. Soc. Rev.*, 2018, **47**, 2431–2453.
4 M. Feng and M. L. Tong, *Chem. – Eur. J.*, 2018, **24**, 7574–7594.
5 F.-S. Guo, A. K. Bar and R. A. Layfield, *Chem. Rev.*, 2019, **119**, 8479–8505.
6 F.-S. Guo, B. M. Day, Y.-C. Chen, M.-L. Tong, A. Mansikkamäki and R. A. Layfield, *Science*, 2018, **362**, 1400–1403.
7 C. A. P. Goodwin, F. Ortu, D. Reta, N. F. Chilton and D. P. Mills, *Nature*, 2017, **548**, 439–442.
8 F. Liu, D. S. Krylov, L. Spree, S. M. Avdoshenko, N. A. Samoylova, M. Rosenkranz, A. Kostanyan, T. Greber, A. U. Wolter and B. Büchner, *Nat. Commun.*, 2017, **8**, 1–9.
9 J. D. Rinehart, M. Fang, W. J. Evans and J. R. Long, *J. Am. Chem. Soc.*, 2011, **133**, 14236–14239.
10 J. D. Rinehart, M. Fang, W. J. Evans and J. R. Long, *Nat. Chem.*, 2011, **3**, 538–542.
11 S. T. Liddle and J. van Slageren, *Chem. Soc. Rev.*, 2015, **44**, 6655–6669.
12 D. Aravena, *J. Phys. Chem. Lett.*, 2018, **9**, 5327–5333.
13 A. Castro-Alvarez, Y. Gil, L. Llanos and D. Aravena, *Inorg. Chem. Front.*, 2020, **7**, 2478–2486.
14 M. J. Giansiracusa, A. K. Kostopoulos, D. Collison, R. E. Winpenny and N. F. Chilton, *Chem. Commun.*, 2019, **55**, 7025–7028.
15 I. F. Díaz-Ortega, J. M. Herrera, Á. Reyes Carmona, J. R. Galán-Mascarós, S. Dey, H. Nojiri, G. Rajaraman and E. Colacio, *Front. Chem.*, 2018, **6**, 537.
16 S. Mukherjee, J. Lu, G. Velmurugan, S. Singh, G. Rajaraman, J. Tang and S. K. Ghosh, *Inorg. Chem.*, 2016, **55**, 11283–11298.
17 S. Ghosh, S. Mandal, M. K. Singh, C.-M. Liu, G. Rajaraman and S. Mohanta, *Dalton Trans.*, 2018, **47**, 11455–11469.
18 I. F. Diaz-Ortega, J. M. Herrera, D. Aravena, E. Ruiz, T. Gupta, G. Rajaraman, H. Nojiri and E. Colacio, *Inorg. Chem.*, 2018, **57**, 6362–6375.

19 P. Evans, D. Reta, C. A. P. Goodwin, F. Ortu, N. F. Chilton and D. P. Mills, *Chem. Commun.*, 2020, **56**, 5677–5680.
20 T. Han, Y.-S. Ding, Z.-H. Li, K.-X. Yu, Y.-Q. Zhai, N. F. Chilton and Y.-Z. Zheng, *Chem. Commun.*, 2019, **55**, 7930–7933.
21 J. Long, F. Habib, P.-H. Lin, I. Korobkov, G. Enright, L. Ungur, W. Wernsdorfer, L. F. Chibotaru and M. Murugesu, *J. Am. Chem. Soc.*, 2011, **133**, 5319–5328.
22 Y.-N. Guo, G.-F. Xu, W. Wernsdorfer, L. Ungur, Y. Guo, J. Tang, H.-J. Zhang, L. F. Chibotaru and A. K. Powell, *J. Am. Chem. Soc.*, 2011, **133**, 11948–11951.
23 S. Demir, M. I. Gonzalez, L. E. Darago, W. J. Evans and J. R. Long, *Nat. Commun.*, 2017, **8**, 1–9.
24 D. Errulat, B. Gabidullin, A. Mansikkamaki and M. Murugesu, *Chem. Commun*, 2020, **56**, 5937–5940.
25 H. Tian, B.-L. Wang, J. Lu, H.-T. Liu, J. Su, D. Li and J. Dou, *Chem. Commun.*, 2018, **54**, 12105–12108.
26 K. L. Harriman, J. J. Le Roy, L. Ungur, R. J. Holmberg, I. Korobkov and M. Murugesu, *Chem. Sci.*, 2017, **8**, 231–240.
27 L. Ungur, M. Thewissen, J.-P. Costes, W. Wernsdorfer and L. F. Chibotaru, *Inorg. Chem.*, 2013, **52**, 6328–6337.
28 E. Ruiz, J. Cano, S. Alvarez and P. Alemany, *J. Comput. Chem.*, 1999, **20**, 1391–1400.
29 W. Huang, J. J. Le Roy, S. I. Khan, L. Ungur, M. Murugesu and P. L. Diaconescu, *Inorg. Chem.*, 2015, **54**, 2374–2382.
30 W.-B. Sun, B. Yan, L.-H. Jia, B.-W. Wang, Q. Yang, X. Cheng, H.-F. Li, P. Chen, Z.-M. Wang and S. Gao, *Dalton Trans.*, 2016, **45**, 8790–8794.
31 M. He, F. S. Guo, J. Tang, A. Mansikkamaki and R. A. Layfield, *Chem. Sci.*, 2020, **11**, 5745–5752.
32 We have divided the QTM/TA-QTM values obtained from ab initio calculation by $1\mu_B$ to obtain unitless value for the equation.